Inorganic Chemistry
Article

Inorg. Chem. **2010**, *49*, 5033–5039 **5033**
DOI: 10.1021/ic100131z

Control of Metal Ion Size-Based Selectivity through Chelate Ring Geometry. Metal Ion Complexing Properties of 2,2′-Biimidazole

David Buist,[†] Neil J. Williams,[†] Joseph H. Reibenspies,[‡] and Robert D. Hancock*,[†]

[†]*Department of Chemistry and Biochemistry, University of North Carolina at Wilmington, Wilmington, North Carolina 28403, and* [‡]*Department of Chemistry, Texas A&M University, College Station, Texas 77843*

Received January 21, 2010

Some metal ion complexing properties of 2,2′-biimidazole (BIM) are presented. The ligand BIM forms minimum steric strain complexes with hypothetical metal ions with M−N (metal−nitrogen) bond lengths of 4.2 Å, in contrast to more usual ligands such as bipy (2,2′-bipyridyl) that prefer metal ions with M−N bond lengths of 2.51 Å. This metal ion size-based preference of BIM suggests that ligands with such architecture could be used to produce selectivity (differences in log K_1) for very large metal ions. To test this hypothesis, the crystal structure of $[Pb(BIM)_2(ClO_4)_2]_2$ (**1**) was determined as the first example of a complex of BIM with a large metal ion. In addition, formation constants (log K_1) for BIM with metal ions ranging from the very small Cu(II) to the very large Ba(II) ion were determined to examine the effect of the architecture of BIM on metal ion selectivity. The structure of **1** gave: Triclinic, $P\bar{1}$, a = 8.314(2) Å, b = 8.677(2) Å, c = 14.181(3) (Å), α = 91.143(3)°, β = 104.066(2)°, γ = 106.044(3)°, V = 949.5(4) Å^3, Z = 1, R = 0.030. Pb(II) in **1** is eight-coordinate, with relatively short Pb−N bonds to the two BIM ligands ranging from 2.366(5) to 2.665(5) Å, while the four Pb−O bonds are very long at 2.826(5) to 3.123(5) Å. This is typical of the structure of Pb(II) complexes that have a stereochemically active lone pair of electrons, which is postulated to be situated in the vicinity of the long Pb−O bonds. The geometry of the chelate rings formed by BIM with Pb(II) in **1** is analyzed, and it is shown that these are closer in structure to the minimum-strain chelate ring formed by BIM with a very large metal ion than is the case for structures reported in the literature with smaller metal ions. The formation constants (log K_1) determined for BIM at 25 °C in 0.1 M $NaClO_4$ by UV−visible spectroscopy are as follows: Cu(II), 6.35; Ni(II), 4.89; Zn(II), 3.42; Cd(II), 3.86; Ca(II), −0.2; Pb(II), 3.2; Ba(II), 0.2. The log K_1 values for BIM complexes show that, as expected from the geometry of the chelate ring formed by BIM, the complexes of BIM with small metal ions such as Cu(II) are considerably weaker than with ligands such as bipy, where the ligand architecture is more favorable for forming chelate rings with small metal ions. In contrast, for very large metal ions such as Pb(II) or Ba(II), the log K_1 values for BIM complexes are larger than for bipy. The use of ligand architecture in BIM-type ligands to engineer selectivity for very large metal ions is discussed. Some fluorescence results for BIM and its complexes are presented. BIM itself fluoresces very strongly, while all of its complexes except for Ca(II) show diminished fluorescence intensity, ranging from small shifts and decreases for Ba(II) to very large decreases for Cd(II), which may be due to the distortion of the ligand geometry in its complexes by metal ions that are too small for low-strain coordination with BIM.

Control of ligand selectivity for metal ions (difference in log K_1 with metal ions of interest) is important in areas such as biomedical,[1] biological,[2] and environmental[3] applications, and in metal ion separations.[4] Particularly important in ligand architecture is the degree of preorganization.[5] Preorganized ligands are constrained to be in the conformation required in the complex formed with a target metal ion. Examples of preorganized ligands are crown ethers,[6] cryptands,[7] and aza-macrocycles,[8] whose macrocyclic structure leads to considerable thermodynamic stabilization[7,8] of complexes formed compared to non-macrocyclic analogues. A dominant aspect of ligand architecture is the size of the chelate ring.[9] Five-membered chelate rings promote selectivity for large metal ions, while 6-membered chelate rings promote selectivity for small metal ions.

The effect of chelate ring size arises from the focus of the lone pairs on the donor atoms in the chelate ring formed by

*To whom correspondence should be addressed. E-mail: hancockr@uncw.edu.

(1) Orvig, C.; Abrams, M. *Chem. Rev.* **1999**, *99*, 2201, and following papers in that issue.
(2) Bencini, A.; Bernardo, M. A.; Bianchi, A.; Garcia-Espana, E.; Giorgi, C.; Luis, S.; Pina, F.; Valtancoli, B. *Adv. Supramol. Chem.* **2002**, *8*, 79.
(3) *Trace Elements in Natural Waters*; Steinnes, E., Salbu, B., Eds.; CRC Press: Boca Raton, FL, 1995.
(4) Gorden, A. E. V.; Xu, J.; Raymond, K. N. *Chem. Rev.* **2003**, *103*, 4207.
(5) Cram, D. J.; Cram, J. M. *Acc. Chem. Res.* **1978**, *11*, 8.
(6) Pederson, C. J. *J. Am. Chem. Soc.* **1967**, *89*(2495), 7017.
(7) Lehn, J. M. *Acc. Chem. Res.* **1978**, *11*, 49.
(8) Cabbiness, D. K.; Margerum, D. W. *J. Am. Chem. Soc.* **1969**, *91*, 6540.
(9) Hancock, R. D.; Martell, A. E. *Chem. Rev.* **1989**, *89*, 1875.

Published on Web 05/06/2010

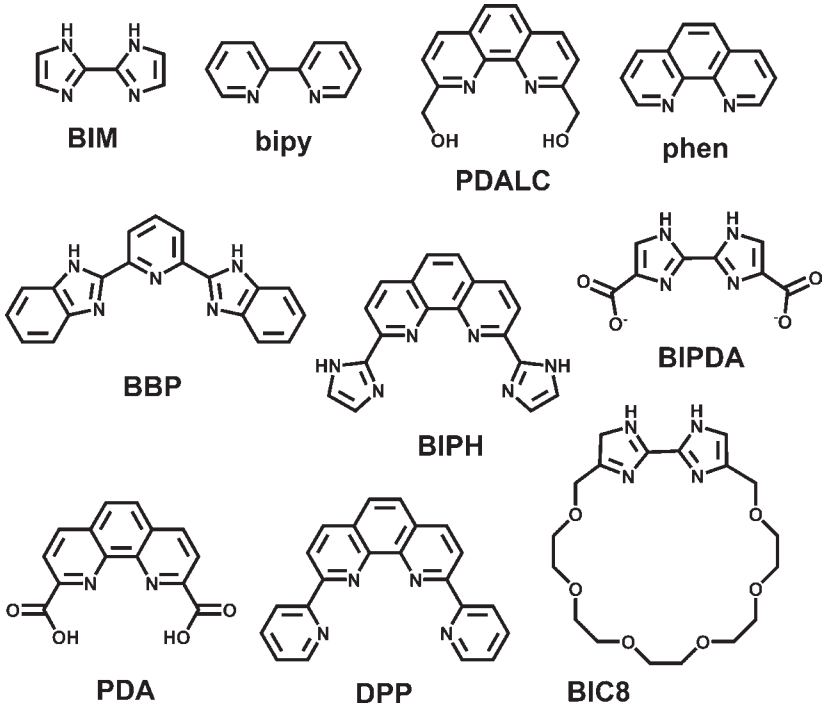

Figure 1. Ligands discussed in this paper.

the ligand. Six-membered chelate rings favor extremely small metal ions, while the typical 5-membered chelate ring forms with least strain with metal ions with an ionic radius[10] (r^+) of about 1.0 Å.

There is some interest in selectively complexing metal ions with radii considerably larger than 1.00 Å, such as ^{82}Rb (r^+ for Rb^+ = 1.52 Å) in PET (positron emission tomography) applications,[11] and ^{135,137}Cs (r^+ for Cs^+ = 1.64 Å) and ^{90}Sr (r^+ for Sr^{2+} = 1.18 Å) in the treatment of nuclear waste.[12,13] In the case of ^{82}Rb, at present the only application in PET is its use for heart perfusion, where the Rb^+ cation mimics K^+ and allows for imaging of the heart. A ligand that selectively complexed Rb^+ would allow for the use of ^{82}Rb in other PET applications where the ideal properties of ^{82}Rb for PET imaging could be utilized. The Pb^{2+} ion is also large (r^+ = 1.19 Å), and might benefit in the treatment of lead intoxication[14] from ligand architecture that favored metal ions with an r^+ larger than 1.0 Å.

In the case of the bipy chelate ring (see Figure 1 for structure of ligands discussed here) the minimum-strain M−N bond length of 2.51 Å is arrived at here using MM (molecular mechanics) calculations.[15,16] MM can be used[15,16] to calculate the strain energy of the complex as a function of M−L (metal−ligand) bond length. The minimum in the curve of U (strain energy) versus M−L bond length is then the best-fit size. The strain energy of the complex $[M(bipy)F_4]^{n-}$ was calculated using the MM+ force field (essentially the MM2[17] force field) present in the program HyperChem.[18] The ideal M−N length was varied from 1.6 to 3.2 Å to generate the curve of U versus M−N in Figure 2. The M−N force constant was kept constant at 0.7 mdyne/Å, which has been found[15,16] to be an adequate representative value. A polynomial (Figure 2) was fitted[19] to the curve of U versus M−N to allow for accurate determination of the minimum of U versus M−N at M−N = 2.51 Å. The metal ion closest to having this geometry is probably Y(III) which has average

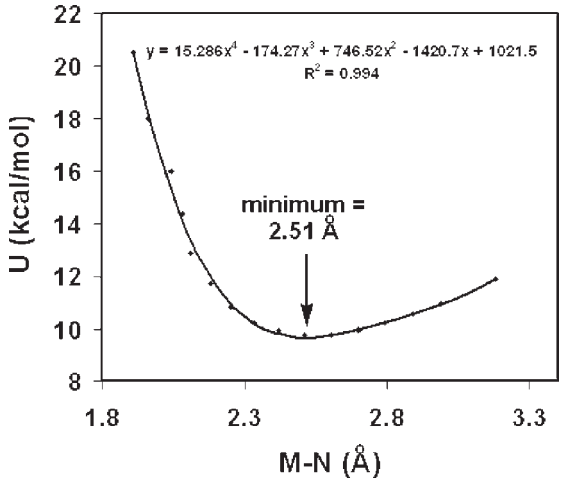

Figure 2. Strain energy (U) for the complex $[M(bipy)F_4]^{n-}$ as a function of energy-minimized M−N length, calculated from MM using the program HyperChem.[18] The minimum in the fitted polynomial at M−N = 2.51 Å is[15,16] the best-fit size M−N length for coordinating with bipy. The equation shown on the diagram is the polynomial which generates the solid line fitted[19] to the calculated points (♦), and which was used to calculate the minimum in the curve at M−N = 2.51 Å.

(10) Shannon, R. D. *Acta Crystallogr., Sect. A* **1976**, *A32*, 751.
(11) Knuuti, J.; Bengel, F. M. *Heart* **2008**, *94*, 360.
(12) Levitskaia, T. G.; Lamb, J. D.; Fox, K. L.; Moyer, B. A. *Radiochim. Acta* **2002**, *90*, 43.
(13) Casnati, A.; Sansone, F.; Dozol, J.-F.; Rouquette, H.; Arnaud-Neu, F.; Byrne, D.; Fuangswasdi, S.; Schwing-Weill, M.-J.; Ungaro, R. *J. Inclusion Phenom. Macrocyclic Chem.* **2001**, *41*, 193.
(14) Andersen, O. *Mini-Rev. Med. Chem.* **2004**, *4*, 11.
(15) Hancock, R. D. *Acc. Chem. Res.* **1990**, *26*, 875.
(16) Hancock, R. D. *Prog. Inorg. Chem.* **1989**, *37*, 187.
(17) Allinger, N. L. *J. Am. Chem. Soc.* **1977**, *98*, 8127.
(18) *Hyperchem program*, version 7.5; Hypercube, Inc.: Waterloo, Ontario, Canada.
(19) Billo, E. J. *EXCEL for Chemists*; Wiley-VCH: New York, 2001.

M−N = 2.513 Å (Cambridge structural database (CSD)[20] 6 structures) in its bipy complexes, typified by the complex $[Y(bipy)(H_2O)_6]^{3+}$.[21] The latter structure shows the H--H non-bonded distance for the H-atoms on the C3 atoms of bipy at about 2.1 Å to be much less than the sum of the van der Waals radii[22] for H-atoms of 2.44 Å. These H--H non-bonded repulsions contribute to the observed chelate ring geometry of bipy chelate rings, making the best-fit M−N length slightly shorter than it would be otherwise. These, and other H--H non-bonded repulsions, are a major factor in the coordination of ligands containing pyridyl groups.[23]

To shift metal ion selectivity in the direction of metal ions with r^+ larger than 1.0 Å, one needs to alter the geometry of the chelate ring so that the lone pairs on the donor atoms are focused at a greater distance than is true for bipy, for example. A candidate ligand for this is BIM (2,2′-biimidazole). Complexes of BIM have been studied structurally, with 109 structures reported in the CSD.[20] However, thermodynamic studies have been limited to a report[24] of the formation constants of BIM with Cu^{2+}, Ni^{2+}, and Zn^{2+}. These are[10] small metal ions, so that log K_1 values for these ions with BIM do not indicate the metal ion size preferences of the ligand. A simple analysis of the chelate ring geometry of BIM complexes is carried out as below, where the lone pairs on the N-donors lie along lines extrapolated from the midpoint of the C−N bond opposite the N-donor, through the N-donor. Such an analysis, as well as MM calculations, suggests that only an extremely large metal ion with M−N = 4.2 Å would form a minimum strain chelate ring with BIM:

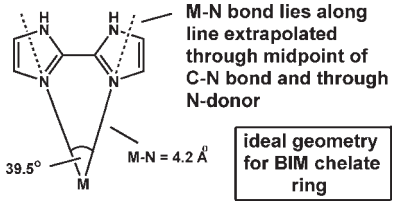

No metal ion is large enough to form such a chelate ring. However, one would expect larger metal ions to be able to adapt better to the steric demands of the BIM chelate ring, and so generate greater selectivity toward large metal ions than does bipy, which, as discussed above, has a best-fit M−N bond length requirement of only 2.51 Å. To assess the selectivity patterns of BIM with larger metal ions, log K_1 values for the large Cd(II) (r^+ = 0.96 Å), Ca(II) (r^+ = 1.00 Å), Ba(II) (r^+ = 1.36 Å), and Pb(II) ions (r^+ = 1.19 Å) with BIM are reported here. Since Ba^{2+} is the largest metal ion (r^+ = 1.36 Å) that seemed likely to form a complex with BIM, its complex-formation was studied by both fluorescence and absorption methods. It was found that the emission spectra were more sensitive than the absorption spectra of BIM to the formation of complexes, so that these were used as a check on the formation constants determined from the absorption spectra. The structures reported[20] for BIM complexes do not include those for any large metal ions, and so to aid in the analysis of the structures of chelate rings of BIM, the structure of $[Pb(BIM)_2(ClO_4)_2]_2$ is reported here.

Table 1. Crystal Data and Structure Refinement for (**1**), $[Pb(BIM)_2(ClO_4)_2]_2$ Complex

empirical formula	$C_{24}H_{24}Cl_4N_{16}O_{16}Pb_2$
formula weight	1348.77
temperature	110(2) K
crystal system	triclinic
space group	$P\bar{1}$
unit cell dimensions	
a (Å)	8.314(2)
b (Å)	8.677(2)
c (Å)	14.181(3)
α (deg)	91.143(3)
β (deg)	104.066(2)
γ (deg)	106.044(3)
volume (Å^3)	949.5(4)
Z	1
reflections collected	7159
independent reflections	3155 [R(int) = 0.0445]
final R indices [$I > 2\sigma(I)$]	R1 = 0.0300, wR2 = 0.0698
R indices (all data)	R1 = 0.0314, wR2 = 0.0704

Experimental Section

Materials and Methods. The ligand BIM (2,2′-biimidazole) was obtained from Matrix-Scientific in 98% purity, and used as received. The metal perchlorates were obtained from VWR or Strem in 99% purity or better, and used as received. All solutions were made up in deionized water (Milli-Q, Waters Corp.) of > 18 MΩ.cm^{-1} resistivity.

Synthesis of $[Pb(BIM)_2(ClO_4)_2]_2$ (1). Crystals of the Pb(II) complex with BIM (**1**) were prepared by dissolving 0.2700 g of BIM in 50.00 mL of hot methanol. To this solution 0.4635 g of $Pb(ClO_4)_2 \cdot 6H_2O$ dissolved in 10.00 mL of methanol was added. Upon addition of the metal salt solution, the cloudy gray ligand solution became a clear light brown. This solution was heated under reflux for 1.5 h and filtered hot. The solution was then allowed to cool and evaporate slowly. After 1 week, fine light-brown needles were collected by filtration. ***Caution!*** *Organic perchlorates may present fire hazards*. Elemental analysis: Calcd. for $C_{12}H_{12}N_8O_8Cl_2Pb$, C, 21.37%; H, 1.79%; N, 16.62%. Found: C, 21.18%; H, 1.76%; N, 16.65%.

Molecular Structure Determination. A mounted crystal of **1** was placed in a cold nitrogen stream maintained at 110 K. A Bruker APEXII four-circle diffractometer was employed for crystal screening, unit cell determination, and data collection. The structures were solved by Patterson synthesis, and refined to convergence.[25] Details of the structure determination of **1** are shown in Table 1, and these together with the crystal coordinates have been deposited with the Cambridge Structural Database (CSD).[20] Some more important bond lengths and angles for **1** are given in Table 2. The structure of **1** is shown in Figure 3.

Formation Constant Determination. These were determined by UV−visible spectroscopy following procedures similar to those reported previously[27,28] for studying complexes of phen-based ligands such as PDALC. UV−visible spectra were recorded using a Varian 300 Cary 1E UV−visible Spectrophotometer controlled by Cary Win UV Scan Application version 02.00(5) software. A VWR sympHony SR60IC pH meter with a VWR sympHony gel epoxy semimicro combination pH electrode was used for all

(20) *Conquest*, 1.12; Cambridge Crystallographic Data Centre: Cambridge, U.K., 2010.
(21) Semenova, L. I.; Skelton, B. W.; White, A. H. *Aust. J. Chem.* **1999**, *52*, 551.
(22) Bondi, A. *J. Phys. Chem.* **1964**, *68*, 441.
(23) Cockrell, G. M.; Zhang, G.; VanDerveer, D. G.; Thummel, R. P.; Hancock, R. D. *J. Am. Chem. Soc.* **2008**, *130*, 1420.
(24) Török, I.; Surdy, P.; Rockenbauer, A.; Korecz, L., Jr.; Anthony, G. J.; Koolhaas, A.; Gajda, T. *J. Inorg. Biochem.* **1998**, *71*, 7.
(25) Gabe, E. J.; Le Page, Y.; Charland, J.-P.; Lee, F. L.; White, P. S. *J. Appl. Crystallogr.* **1989**, *22*, 384.
(26) *ORTEP-3 for Windows*, Version 1.08; Farrugia, L. J. *J. Appl. Crystallogr.* **1997**, *30*, 565.
(27) Gephart, R. T., III; Williams, N. J.; Reibenspies, J. H.; De Sousa, A. S.; Hancock, R. D. *Inorg. Chem.* **2008**, *47*, 10342.
(28) Gephart, R. T., III; Williams, N. J.; Reibenspies, J. H.; De Sousa, A. S.; Hancock, R. D. *Inorg. Chem.* **2009**, *48*, 8201.

Table 2. Selection of More Important Bond Angles and Lengths[a] for (**1**), $[Pb(BIM)_2(ClO_4)_2]_2$

Bond Lengths (Å)			
Pb(1)−N(7)	2.366(5)	Pb(1)−N(1)	2.474(5)
Pb(1)−N(3)	2.582(5)	Pb(1)−N(5)	2.665(5)
Pb(1)−O(11)	2.826(5)	Pb(1)−O(23)	3.079(5)
Pb(1)−O(41)′	2.952(5)	Pb(1)−O(13)	3.123(5)
Bond Angles (deg)			
N(7)−Pb(1)−N(1)	90.73(16)	N(7)−Pb(1)−N(3)	76.17(15)
N(1)−Pb(1)−N(3)	67.59(16)	N(7)−Pb(1)−N(5)	67.33(15)
N(1)−Pb(1)−N(5)	74.95(15)	N(3)−Pb(1)−N(5)	126.47(15)

[a] The apostrophe indicates that the O-atom in the Pb(1)−O(14)′ bond is bridging from an adjacent Pb atom in the $[Pb(BIM)_2(ClO_4)_2]_2$ dimer.

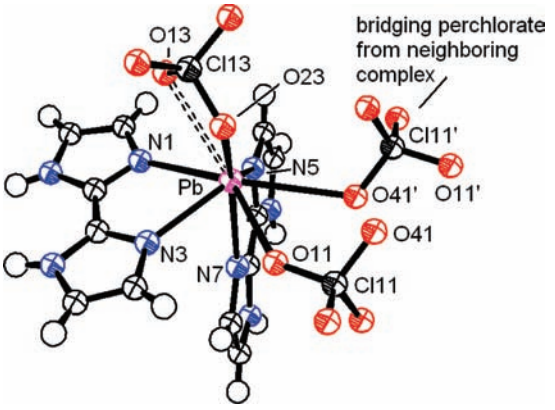

Figure 3. Structure of one $[Pb(BIM)_2(ClO_4)_2]$ half of the centrosymmetric perchlorate-bridged dimer in **1**, showing the numbering scheme for atoms coordinated to Pb. Thermal ellipsoids not shown. Drawing made with ORTEP.[26]

pH readings, which were made in the external titration cell, with N_2 bubbled through the cell to exclude CO_2. The pH meter was calibrated prior to each titration, by means of titration of standard acid with standard base: the value of $E°$ for the cell, as well as the Nernstian slope, was obtained from a linear plot of measured values of E versus the calculated pH. The cell containing 50 mL of ligand/metal solution was placed in a bath thermostatted to 25.0 ± 0.1 °C, and a peristaltic pump was used to circulate the solution through a 1.0 cm quartz flow cell situated in the spectrophotometer. The pH was altered in the range 2 to 12 by additions to the external titration cell of small amounts of standard $HClO_4$ or NaOH as required using a micropipet. After each adjustment of pH, the system was allowed to mix by operation of the peristaltic pump for 15 min prior to recording the spectrum, and to ensure proper mixing, the solution in the external cell was agitated with a magnetic stirrer.

The protonation constant of BIM was determined by recording the spectra of a 2.50×10^{-5} M solution in 0.1 M $NaClO_4$ at a range of pH values. The spectra in the pH range 3.24 to 6.76 are shown in Figure 5 The variation in absorbance at five different wavelengths was fitted to a single protonation constant of $pK = 5.15 \pm 0.03$. The fitting was carried out using EXCEL,[19] and the standard deviation was determined using the SOLVSTAT macro available in reference 19. Formation constants for the metal ions were obtained by repeating the above titrations in the presence of 1:1 concentrations of the metal ion and BIM (3.50×10^{-5} *M*). The log K_1 values were obtained by fitting the spectra using EXCEL and obtaining a constant for the equilibrium:

$$M(BIM)^{2+} + H^+ \leftrightarrows BIMH^+ + M^{2+} \quad (1)$$

Table 3. Formation Constants for BIM (2,2′-biimidazole)[a]

Lewis acid	equilibrium	log K	ionic strength	reference
H^+	$H^+ + OH^- \leftrightarrows H_2O$	13.78	0.1	29
	$BIM + H^+ \leftrightarrows BIMH^+$	5.15(3)	0.1	this work
		5.19(3)	0.1	24
		5.21(3)	1.0	this work
Cu^{2+}	$Cu^{2+} + BIM \leftrightarrows Cu(BIM)^{2+}$	6.35(6)	0.1	this work
		6.27(4)	0.1	24
Ni^{2+}	$Ni^{2+} + BIM \leftrightarrows Ni(BIM)^{2+}$	4.89(6)	0.1	this work
		4.87(3)	0.1	24
Zn^{2+}	$Zn^{2+} + BIM \leftrightarrows Zn(BIM)^{2+}$	3.42(6)	0.1	this work
		3.48(3)	0.1	24
Cd^{2+}	$Cd^{2+} + BIM \leftrightarrows Cd(BIM)^{2+}$	3.86(6)	0.1	this work
Ca^{2+}	$Ca^{2+} + BIM \leftrightarrows Ca(BIM)^{2+}$	−0.2(1)	0.1	this work
Pb^{2+}	$Pb^{2+} + BIM \leftrightarrows Pb(BIM)^{2+}$	3.20(6)	0.1	this work
Ba^{2+}	$Ba^{2+} + BIM \leftrightarrows Ba(BIM)^{2+}$	0.2(1)	1.0	this work

[a] In 0.1 M $NaClO_4$ or in 1.0 M $NaClO_4$ at 25 °C, as indicated.

This constant could then be combined with the pK value for BIM to obtain log K_1. The variation of 2×10^{-5} M BIM plus Ni^{2+} is seen in Figure 6.The equilibrium constants measured here for BIM are seen in Table 3. The log K_1 values for the BIM complexes of Cu(II), Ni(II), and Zn(II) are in reasonable agreement with those reported previously.[24]

Fluorescence Measurements. Emission spectra (ES) fluorescence properties were determined on a Horiba Jobin Yvon Fluororlog-3 scanning fluorometer equipped with a 450 W Xe short arc lamp and a R928P detector. The instrument was configured to collect the signal in ratio mode with dark offset using 5 nm bandpasses on both the excitation and the emission monochromators. The ES were determined by measurements every 5 nm from 335 to 480 at 245 nm excitation wavelength. Scans were corrected for instrument configuration using factory supplied correction factors. Post processing of scans was performed using the FluorEssence program.[30] The software eliminates Rayleigh and Raman scattering peaks by excising portions (±10−15 nm FW) of each scan centered on the respective scatter peak. Following removal of scatter peaks, data were normalized to a daily determined water Raman intensity (275ex/303em, 5 nm band-passes). Replicate scans were generally within 5% agreement in terms of intensity and within band-pass resolution in terms of peak location. The ES of 2.0×10^{-5} M BIM plus a selection of M(II) BIM complexes as a function of pH were recorded in a STARNA model 71FQ10 quartz fluorescence flow-cell connected to a titration vessel and peristaltic pump as described for the absorption measurements.

Results and Discussion

Structure of $[Pb(BIM)_2(ClO_4)_2]_2$ (1). The structure of one $[Pb(BIM)_2(ClO_4)_2]$ half of the centrosymmetric perchlorate-bridged dimer in **1** is seen in Figure 3. The Pb may be described as 8-coordinate with the four N-donors of the two BIM ligands at Pb−N distances ranging from 2.366(5) to 2.665(5) Å, which can be compared with bonds of 2.417 and 2.663 Å reported for Pb(II) complexes with imidazoles (two structures[31,32]) in the CSD.[20] The four Pb−O bonds to the perchlorates, one of which is bridging between two $[Pb(BIM)_2(ClO_4)_2]$ units, are much longer, ranging from 2.826(5) to 3.123(5) Å. This is

(29) Martell, A. E.; Smith, R. M. *Critical Stability Constant Database, 46*; National Institute of Science and Technology (NIST): Gaithersburg, MD, 2003.
(30) *FluorEssence program, version 2.1*; HORIBA Jobin Yvon, Inc.: Edison, NJ.
(31) Hamilton, B. M.; Ziegler, C. J. *Inorg. Chem.* **2004**, *43*, 4272.
(32) Hamilton, B. H.; Wagler, T. A.; Espe, M. P.; Ziegler, C. J. *Inorg. Chem.* **2005**, *44*, 4891.

typical[33−35] of complexes with stereochemically active lone pairs of electrons on the Pb(II). The less electronegative donor atoms (the N-donors in this case) occupy the site opposite the lone pair, and form short Pb−L (L = ligand) bonds, while the more electronegative O-donors occupy sites closer to the postulated position of the lone pair, and form long Pb−L bonds.

Of particular interest here is how the large Pb(II) ion coordinates with BIM, in view of the requirement of BIM, discussed above, for a very large metal ion to form a minimum strain chelate ring. It has been shown[36] that for any one chelating ligand, one can obtain a good relationship between the M−L bond lengths of the complexes, and the L−M−L bond angles. Such systematic structural responses to variation in metal ion size provide a basis for understanding the relationships between metal ion size and metal ion size-based selectivities based on such architectural features as chelate ring size.[9]

In Figure 4a is shown the relationship between N−M−N bond angle and M−N length for 109 complexes of BIM reported in the CSD,[20] as well as the Pb(II) complex reported here, and also includes the dimensions of the minimum-strain chelate ring of BIM involving a metal ion with M−N bond lengths of 4.2 Å, as determined by MM calculation. The large Pb(II) ion gets a little closer to the minimum strain geometry of the BIM chelate ring, but there is much scope for an even larger metal ion such as Cs^+ (Cs−N bond lengths average 3.22 ± 0.14 Å, CSD[20] 84 structures) to bond with BIM-type ligands in a low-strain manner. Plots such as seen in Figure 4a can also involve other structural parameters of the chelate ring as a function of M−L bond length, although these are usually not as clear-cut as those involving L−M−L bond angles. In Figure 4b is shown the dependence of the N−C−C angle within the BIM chelate rings (shown on the diagram) on M−N bond length. It is interesting to see how the complex responds to the fact that the metal ions may be too small to coordinate in a low-strain manner. As the metal ion becomes smaller, simple geometric arguments would suggest that the M−N−C angles would become much smaller than the ideal value of 126° expected in the minimum strain ring. This deformation of the chelate ring is partly relieved by compression of the N−C−C angle away from its ideal value of 126°, which compression becomes more marked as the metal ion becomes smaller. It is interesting to note that the M−N−C angles in the BIM complexes change with varying M−N length, and it is in fact the N−C−C angles within the BIM chelate ring that bend to accommodate smaller metal ions. The structure of $[Pb(BIM)_2(ClO_4)_2]$ suggests that the large Pb(II) ion is a better fit for the BIM chelate ring, so that the interest is then to see how this influences the metal ion size-based selectivity of BIM.

Formation Constants and Metal Ion Selectivity of BIM. In Figure 5 is seen the variation in the absorption spectra

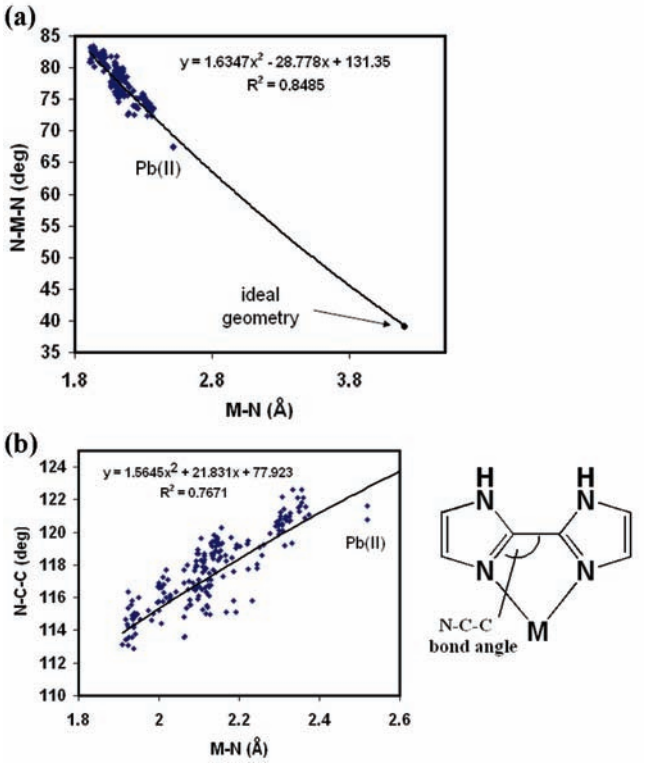

Figure 4. (a) Relationship between N−M−N bond angle and M−N bond length for chelate rings involving BIM. Structural data from CSD[20] (109 structures) except for Pb(II) complex, this work. The ideal geometry for a minimum strain chelate ring involving the BIM ligand indicated on the diagram was estimated as discussed in the text. (b) Relationship between N−C−C bond angle and M−N bond length for chelate rings involving BIM. Structural data from CSD[20] (109 structures) except for Pb(II) complex, this work. The N−C−C angle in the ideal chelate ring involving BIM should be 126° from MM calculation.

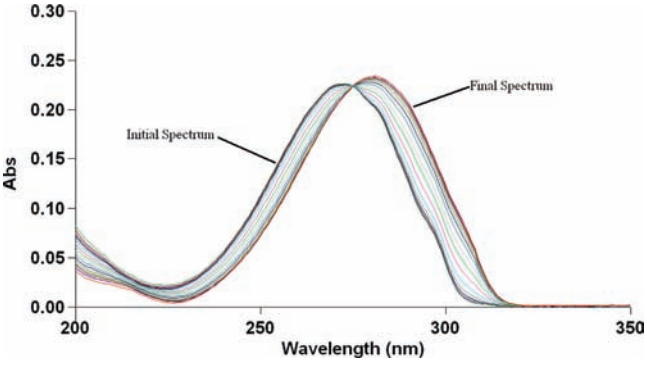

Figure 5. Variation of spectra of 2.50×10^{-5} M BIM in 0.1 M $NaClO_4$ as a function of pH from pH = 6.76 (initial spectrum) to pH = 3.24 (final spectrum). The isosbestic point is at 275 nm.

of BIM as a function of pH, and in Figure 6 is seen the variation in the absorption spectra as a function of pH of a 1:1 mixture of BIM and Ni^{2+}. The variations in absorbance in these spectra were used to determine the protonation constant and formation constants for BIM, as described above. These formation constants, together with some literature values,[24] are seen in Table 3. It may at first sight be a little surprising that the protonation constant of BIM at 5.15 is considerably less than that of imidazole itself[29] at 7.00. It seems possible that this is due to electrostatic repulsion between the protons

(33) Shimoni-Livny, L.; Glusker, J. P.; Bock, C. W. *Inorg. Chem.* **1998**, *37*, 1853.
(34) Hancock, R. D.; Shaikjee, M. S.; Dobson, S. M.; Boeyens, J. C. A. *Inorg. Chim. Acta* **1988**, *154*, 229.
(35) Hancock, R. D.; Reibenspies, J. H.; Maumela, H. *Inorg. Chem.* **2004**, *43*, 2981.
(36) Hancock, R. D.; Melton, D. L.; Harrington, J. M.; McDonald, F. C.; Gephart, R. T.; Boone, L. L.; Jones, S. B.; Dean, N. E.; Whitehead, J. R.; Cockrell, G. M. *Coord. Chem. Rev.* **2007**, *251*, 1678.

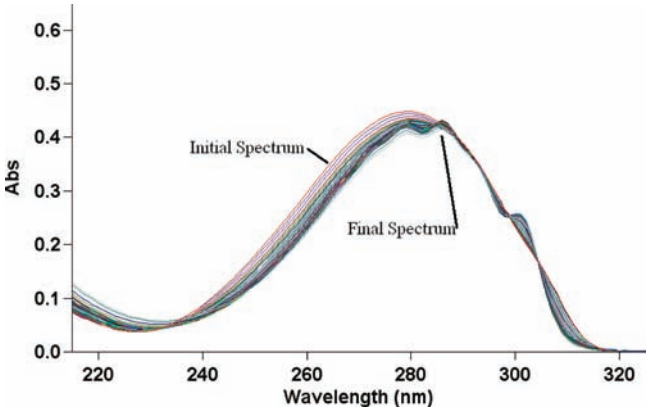

Figure 6. Variation of absorption spectra of 4.50×10^{-5} M BIM in 0.1 M $NaClO_4$ in the presence of 4.50×10^{-4} M Ni^{2+}, as a function of pH from pH = 2.16 (initial spectrum) to pH = 8.54 (final spectrum). The small sharp peaks developed on the final spectra at higher pH may be vibrations coupled to the $\pi-\pi^*$ transitions of BIM in the Ni(II)/BIM complex, as discussed in the text.

Table 4. Comparison of log K_1 Values for BIM (This Work) and bipy Complexes,[29] at Ionic Strength 0.1 and 25 °C

metal ion	r^+ (Å)[a]	log K_1 (BIM)	log K_1 (bipy)	difference
Cu^{2+}	0.57	6.35	8.12	−1.77
Ni^{2+}	0.69	4.89	7.04	−2.15
Zn^{2+}	0.74	3.42	5.12	−1.70
Cd^{2+}	0.96	3.86	4.24	−0.38
Ca^{2+}	1.00	−0.2	−0.1	−0.1
Pb^{2+}	1.19	3.20	3.1	+0.1
Ba^{2+}	1.36	0.2	−0.3	+0.5

[a] Octahedral radii, except for Cu(II), which is the square-planar radius.

on the N-atoms of the adjacent imidazole groups of $BIMH^+$. The formation constants for Cu(II), Zn(II), and Ni(II) with BIM are in reasonable agreement with those reported[24] earlier (Table 3). What is of interest is a comparison of log K_1 values for the BIM complexes with those[29] for bipy (Table 4). The change in complex stability in passing from the bipy complex to the BIM complex as a function of metal ion size is seen in Figure 7. Figure 7 shows that there is a reasonable relationship between metal ion size and the selectivity for BIM relative to bipy, which supports the idea that a chelate ring with the geometry presented by BIM will move selectivity in the direction of much larger metal ions than generated by usual five-membered chelate rings. One sees in Figure 7 that the point for Cu(II) is displaced slightly upward, as though it were larger than suggested by its[10] square-planar radius. The structure[37] for five-coordinate Cu(II) with one BIM shows that one of the N-donors of BIM occupies the axial coordination site on Cu(II), with a long Cu−N bond length, showing how the small Cu(II) has accommodated the requirement of BIM for a larger metal ion.

A point of interest in Figure 6 is the appearance of several small sharp peaks on the absorbance spectrum of the Ni(II)/BIM complex at higher Ni^{2+} concentration. These small peaks are typical of smaller metal ions such as Cu(II), Ni(II), and Zn(II), but are absent in the complexes

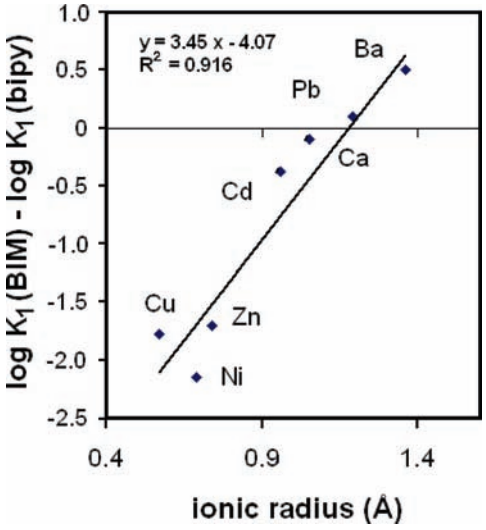

Figure 7. Relationship between difference in log K_1 for BIM complexes and the corresponding bipy complexes,[29] and the ionic radii[10] of the metal ions.

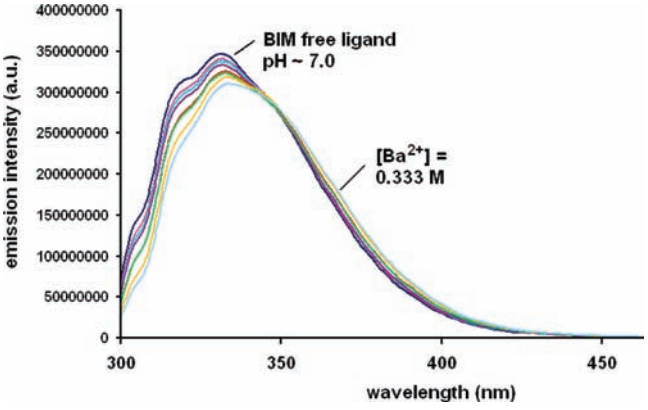

Figure 8. Fluorescence spectrum of 1.0×10^{-5} M BIM in 1.0 M $NaClO_4$, excitation wavelength = 245 nm, as a function of Ba^{2+} concentration.

of BIM with larger metal ions such as Cd(II) or Pb(II). Such small sharp peaks are typical of the complexes of PDA[38] and DPP,[23] although for the latter ligands these are found for the complexes of larger metal ions and not small metal ions. It is possible that vibrations[23,38] involving the greatly stiffened BIM ligand in its complexes with small metal ions become coupled to the $\pi-\pi^*$ transitions of BIM, leading to the structure seen on these transitions as in Figure 6.

Fluorescence. The free ligand BIM fluoresces quite strongly, with a peak at 330 nm at higher pH, and excitation wavelength 245 nm, which emission peak shifts to 345 nm at lower pH. The changes in emission intensity with pH are consistent with a protonation constant of 5.20 at ionic strength about 0. The main purpose here was to use the fluorescence of BIM to obtain additional evidence for the formation of complexes with Ca(II) and Ba(II), as the changes in the absorption spectra of BIM produced by complex-formation with these metal ions was rather small. In Figure 8 is seen the effect of increasing Ba^{2+} concentration on the fluorescence of BIM at pH 7.0, and the shifts, with an isosbestic point at 347 nm, are consistent with a single equilibrium with

(37) Bencini, A.; Mani, F. *Inorg. Chim. Acta* **1988**, *154*, 215.
(38) Williams, N. J.; Dean, N. E.; VanDerveer, D. G.; Luckay, R. C.; Hancock, R. D. *Inorg. Chem.* **2009**, *48*, 7853.

$\log K_1 = 0.2$ for the Ba(II) complex of BIM. In response to a comment from a reviewer, it should be pointed out that the Ba(II)/BIM fluorescence was recorded in a background of 1.0 M $NaClO_4$, so that the changes in the fluorescence spectrum in Figure 8 as a function of Ba^{2+} concentration are not likely to be due to variation in perchlorate concentration. In addition, the fluorescence spectrum of free BIM in 1.0 M $NaClO_4$ background and in pure water is very similar, suggesting that perchlorate has little effect on the fluorescence spectrum of BIM. Perhaps a little surprisingly, Zn(II) produced only a small decrease in emission intensity in BIM on complex-formation, whereas Cd(II) (see Supporting Information) produced a very large decrease in emission intensity for BIM. From observations[38−40] on the intensity of the CHEF (chelation enhanced fluorescence) effect it appears that metal ions that are geometrically ill-suited for formation of a chelate ring with a particular ligand lead to poor overlap in the M−L bond, and hence leave electron density available for quenching the CHEF effect. Only Ca^{2+} of the metal ions studied here produced a small positive CHEF effect with BIM. What is perhaps a little surprising is that the large Cd^{2+} ion produces a large decrease in fluorescence intensity (see Supporting Information), whereas the small Zn(II) ion produces only a small decrease in fluorescence intensity. One would normally expect[41] from the greater spin−orbit coupling effects in heavy metal ions that Cd(II) would, all else being equal, produce a somewhat smaller CHEF effect than Zn(II). However, it has been found[39,40] that ligands that are sterically ill-matched for small metal ions usually lead to a larger CHEF effect in Cd(II) than Zn(II). It may be here that both Zn(II) and Cd(II) are so ill-suited sterically for coordination with BIM that the factors determined previously[38−40] do not apply.

Conclusions

Simple geometric considerations suggest that the ligand BIM would complex with the least strain with the largest possible metal ions. The crystal structure of $[Pb(BIM)_2(ClO_4)_2]_2$ (**1**), in which Pb(II) is the first available structure of a BIM complex with a large metal ion, suggests that the Pb(II) complexes with less steric strain than do the other small metal ions so far studied. The formation constants ($\log K_1$) for BIM complexes show, as would be expected from its predicted preference for very large metal ions, that BIM forms less stable complexes with small metal ions such as Cu(II) and Zn(II) than does bipy. In contrast, BIM forms more stable complexes than does bipy with very large metal ions such as Pb(II) or Ba(II). This preference of BIM for very large metal ions suggests that ligands such as BIPH, BIC8, or BIMDA (Figure 1) might form complexes of high complex stability and very strong selectivity for the very largest metal ions. The ligand BBP (Figure 1) has been studied[42−44] mainly from the point of view of the photophysical properties of its complexes, but it incorporates imidazole groups that lead to an affinity for the largest metal ions (MM indicates a minimum-strain M−N of about 3.0 Å), which suggests a strategy for ligand design for large metal ions, namely combining pyridyl and imidazole groups in chelate rings, as is the case with BBP and BIPH.

Acknowledgment. The authors thank the University of North Carolina Wilmington and the Department of Energy (Grant DE-FG07-07ID14896) for generous support for this work.

Supporting Information Available: Fluorescence spectra of BIM and crystallographic data in CIF format. This material is available free of charge via the Internet at http://pubs.acs.org.

(39) Gan, W.; Jones, S. B.; Reibenspies, J. H.; Hancock, R. D. *Inorg. Chim. Acta* **2005**, *358*, 3958.
(40) Williams, N. J.; Gan, W.; Reibenspies, J. H.; Hancock, R. D. *Inorg. Chem.* **2009**, *48*, 1407.
(41) Berberan-Santos, M. N. *Phys. Chem. Comm.* **2000**, *3*, (on-line) no pages given, article no. 5.
(42) Escande, A.; Guenee, L.; Buchwalder, K.-L.; Piguet, C. *Inorg. Chem.* **2009**, *48*, 1132.
(43) Choi, D.; Kim, T.; Reddy, S. M.; Kang, J. *Inorg. Chem. Commun.* **2009**, *12*, 41.
(44) Meng, F.-Y.; Zhou, Y.-L.; Zou, H.-H.; Zeng, M.-H.; Liang, H. *J. Mol. Struct.* **2009**, *920*, 238.